Hydrazine Nitrosation of a Metal-Bound Nitric Oxide: Structural Evidence for the Formation of an Ammine Complex

Raju Prakash,*,†,§ Andreas W. Götz,⊥ Frank W. Heinemann,† Andreas Görling,⊥ and Dieter Sellmann†,‡

Institut für Anorganische Chemie, Universität Erlangen-Nürnberg, Egerlandstrasse 1,
D-91058 Erlangen, Germany, and Lehrstuhl für Theoretische Chemie,
Universität Erlangen-Nürnberg, Egerlandstrasse 3, D-91058 Erlangen, Germany

Received January 18, 2006

Hydrazine nitrosation of [Ru(NO)(py^{si}S$_4$)]Br·THF (**1**) (py^{si}S$_4{}^{2-}$ = 2,6-bis(3-triphenylsilyl-2-sulfanylphenylthiomethyl)-pyridine^{2-}) in methanol/DMF led to the formation of mononuclear ammine complex [Ru(NH$_3$)(py^{si}S$_4$)] (**2**) and N$_2$O, whereas the reaction performed in THF/CH$_2$Cl$_2$/toluene afforded thioether-bridged dinuclear ammine complex [(NH$_3$)-Ru(μ-py^{si}S$_4$)Ru(py^{si}S$_4$)] (**3**). Compound **2** dimerizes in solution at room temperature to form **3** and is regenerated upon treatment of **3** with NH$_3$. A plausible mechanism for the hydrazine nitrosation of **1** has been proposed. The reaction of **1** with NH$_3$ or N$_3{}^-$ does not lead to a nucleophilic attack at the NO$^+$ ligand but to a deprotonation that yields neutral nitrosyl complex [Ru(NO){py^{si}S$_4$(H$^+$)}] (**4**), which is supported by density functional theory calculations.

Introduction

The electrophilic reaction of nitrogen monoxide (NO) at the transition-metal centers of designed complexes is currently a topic of great significance, particularly because of their fundamental chemical interest in relation to various important biological and environmental processes.[1,2] The transition metal nitrosyl complexes generally possess an electronically delocalized [M−N−O] moiety, with the N atom being the site for the nucleophilic addition.[3] The nucleophilic reaction of hydrazine with NO$^+$ to undergo nitrosation has been well thought out in the in vitro studies of dissimilatory nitrite reductases.[4] The reactivity of hydrazine toward simple compounds as well as metal complexes is of much interest even at the mechanistic level, because it acts as a one-, two-, or four-equivalent reducing agent

depending on the reaction conditions.[5] The reaction between nitrous acid and hydrazine in aqueous solution is known to be a normal N-nitrosation.[6] Stedman proposed two parallel routes for the decomposition of the *N*-nitrosohydrazine intermediate:[6a,b] the first route led to the formation of HN$_3$ and H$_2$O, which is analogous to the well-established mechanism of the diazotization of aromatic amines in moderately concentrated mineral acid solutions,[6c] and obtained a 100% yield of HN$_3$ at high acidities; the second route led to the formation of NH$_3$ and N$_2$O exclusively at low acidities.

* To whom correspondence should be addressed. E-mail: raju.prakash@chemie.uni-erlangen.de.

† Institut für Anorganische Chemie.

§ Current address: Institut für Organische Chemie, Universität Erlangen-Nürnberg, Henkestrasse 42, D-91054 Erlangen, Germany.

⊥ Lehrstuhl für Theoretische Chemie.

‡ Deceased: May 6, 2003.

(1) (a) Richter-Addo, G. B.; Legzdins, P. *Metal Nitrosyls*; Oxford University Press: New York, 1992. (b) Stamler, J. S.; Singel, D. J.; Loscalzo, J. *Science* **1992**, *258*, 1989−1902. (c) Snyder, S. H. *Science* **1992**, *257*, 494−496. (d) Feelisch, M.; Stamler, J. S. In *Methods in Nitric Oxide Research*; Feelisch, M., Stamler, J. S., Eds.; Wiley: Chichester, U.K., 1996, and references therein. (e) *Nitric Oxide, Principles and Actions*; Lancaster, J., Jr., Ed.; Academic Press: New York, 1996.

(2) (a) Hayton, T. W.; Legzdins, P.; Sharp, W. B. *Chem. Rev.* **2002**, *102*, 935−991. (b) Ford, P. C.; Lorkovic, I. M. *Chem. Rev.* **2002**, *102*, 993−1017. (c) Wasser, I. M.; de Vries, S.; Moënne-Loccoz, P.; Schröder, I.; Karlin, K. D. *Chem. Rev.* **2002**, *102*, 1201−1234. (d) Lopez, J. P.; Heinemann, F. W.; Prakash, R.; Hess, B. A.; Horner, O.; Jeandey, C.; Oddou, J.-L.; Latour, J.-M.; Grohmann, A. *Chem.−Eur. J.* **2002**, *8*, 5709−5722. (e) Clarke, M. J. *Coord. Chem. Rev.* **2003**, *236*, 209−233. (f) McCleverty, J. A. *Chem. Rev.* **2004**, *104*, 403−418. (g) Afshar, R. K.; Patra, A. K.; Olmstead, M. M.; Mascharak, P. K. *Inorg. Chem.* **2004**, *43*, 5736−5743. (h) Böttcher, H.-C.; Graf, M.; Mereiter, K.; Kirchner, K. *Organometallics* **2004**, *23*, 1269−1273. (i) Roncaroli, F.; van Eldik, R.; Olabe, J. A. *Inorg. Chem.* **2005**, *44*, 2781−2790. (j) Sauaia, M. G.; de Lima, R. G.; Tedesco, A. C.; da Silva, R. S. *Inorg. Chem.* **2005**, *44*, 9946−9951.

(3) Bottomley, F.; Grein, F. *J. Chem. Soc., Dalton Trans.* **1980**, 1359−1367.

(4) (a) Kim, C. H.; Hollocher, T. C. *J. Biol. Chem.* **1984**, *259*, 2092−2099. (b) Averill, B. A. *Chem. Rev.* **1996**, *96*, 2951−2964.

(5) Stanbury, D. M. *Prog. Inorg. Chem.* **1998**, *47*, 511−561.

(6) (a) Perrot, J. R.; Stedman, G.; Uysal, N. *J. Chem. Soc., Dalton Trans.* **1976**, 2058−2064. (b) Doherty, A. M. M.; Howes, K. R.; Stedman, G.; Naji, M. Q. *J. Chem. Soc., Dalton Trans.* **1995**, 3103−3107. (c) Challis, B. C.; Ridd, J. H. *J. Chem. Soc.* **1962**, 5208.

There are some reports available on the reaction of hydrazine with transition metal nitrosyls.[7−10] However, they show different reaction modes depending on the metal as well as coligand environment, which lead to the formation of different products. To date, only one report describes the nucleophilic reaction of hydrazine with metal-bound NO^+ ($[Fe(CN)_5(NO)]^{2−}$) in aqueous solution to yield ammonia and nitrous oxide exclusively, according to Stedman's second route.[7d] On the other hand, the reactivity of ruthenium nitrosyls with hydrazine reported so far in the literature yielded predominantly metal-bound azide and H_2O.[8] The reaction of $[Ru(NO)(NH_3)_5]^{3+}$ with hydrazine gave N_2O and N_2, but no ammonia was found.[9] It has been reported recently that sulfur-rich ruthenium complex $[Ru(NO)(Et_2NpyS_4)]Br$ ($Et_2NpyS_4{}^{2−}$ = 2,6-bis(2-sulfanylphenylthiomethyl)-4-diethylaminopyridine$^{2−}$) interacts with an excess of hydrazine to form $[Ru(N_2H_4)(EtNpyS_4)]$.[10a] Later, it was confirmed by IR spectroscopy that the hydrazine complex is formed via the intermediate azide complex by ligand exchange.[10b]

In our previous work, we have synthesized a ruthenium nitrosyl complex, $[Ru(NO)(py^{si}S_4)]Br \cdot THF$ (**1**) ($py^{si}S_4{}^{2−}$ = 2,6-bis(3-triphenylsilyl-2-sulfanylphenylthiomethyl)-pyridine$^{2−}$), that contains two sterically bulky $SiPh_3$ groups ortho to the thiolate donors.[11] This {Ru−NO}^{6} nitrosyl (according to the notation of Enemark and Feltham[12]) is photolabile in methanol and releases NO under visible light irradiation to form $[Ru(Br)(py^{si}S_4)]$. Treatment of the bromo derivative with NO in methanol generates **1**, without any side reaction. In the course of a more-detailed study on the reactivity of **1** toward various nucleophiles, we report herein the nitrosation reaction of **1** with hydrazine in different nonaqueous solvents to form nitrous oxide and $[Ru(NH_3)-(py^{si}S_4)]$ (**2**). The latter complex dimerizes in solution to afford a very stable thioether-bridged dinuclear ammine complex $[(NH_3)Ru(\mu-py^{si}S_4)Ru(py^{si}S_4)]$ (**3**). We furthermore describe the reactivity of **1** with ammonia and azide in various organic solvents that results in deprotonation product $[Ru(NH_3)\{py^{si}S_4(H^+)\}]$ (**4**).

Experimental Section

Materials and Methods. All reactions and manipulations were performed under a dinitrogen atmosphere using standard Schlenk

techniques. Reactions with hydrazine were carried out in the dark using a Schlenk tube (volume = 100 mL) fitted with a gastight rubber septum, unless stated otherwise. Solvents were dried under dinitrogen from appropriate drying agents and distilled prior to use. The hydrazine (1 M solution in THF) was purchased from Aldrich Chemicals Co. and used as received. Compound **1** was synthesized as described in our earlier communication.[11] Physical measurements were performed with the following instruments: IR (KBr disks or CaF_2 cuvettes with solvent bands were compensated), Perkin−Elmer 983, 1620 FT-IR, and 16PC FT-IR. NMR: JEOL JNM-GX 270, JEOL JNM-EX 270, or Lambda LA 400 with the residual signals of the deuterated solvent used as an internal reference. Chemical shifts are quoted in the parts per million scale (downfield shifts are positive). Elemental analysis: Carlo Erba EA 1106 or 1108 analyzer. Mass spectra: JEOL MSTATION 700 spectrometer. Gas chromatography/mass spectrometry: Thermo Finnigan MAT 95 XP gas chromatograph/mass spectrometer coupled to a high sensitive split/splitless injector. A separate helium supply was regulated by a mass flow controller. The gas samples were taken from the Schlenk tube before the addition of hydrazine as well as at the end of the reaction by means of a 250 μL gastight syringe. The entire contents of the syringe were injected into the 20 μL loop in order to enhance sample-to-sample reproducibility, and the analysis was repeated three times. The gas separations were accomplished with a fused silica capillary (30 mm × 0.25 mm; 0.25 μm film thickness) column OPTIMA-5 (inner diameter 0.25 μm). The helium gas flow rate was 0.7 mL/min, and the temperature at the injector, interface, and column was kept at 50 °C. The separated gases were analyzed consecutively by positive ion electron impact (EI) mass spectra mode. Cyclic voltammetry: EG&G Princeton Applied Research (PAR) model 264A potentiostat coupled with a conventional three-electrode cell-assembly consisting of a glassy carbon working electrode, a platinum wire reference electrode, and a platinum rod counter electrode. Measurements were made with ca. 1 × $10^{−3}$ M solutions of the complexes in CH_2Cl_2, using 0.1 M tetrabutylammonium hexafluorophosphate as a supporting electrolyte. Ferrocene was used as an internal standard {$E_{1/2}(F_c/F_c{}^+)$ = +410 mV vs NHE (normal hydrogen electrode);[13] scan speeds: 10−200 mV s^{-1}: T = 20 °C. The reversibility and the number of electrons involved in the redox processes were evaluated on the basis of their (ΔE and $E_p − E_{p/2}$) similarity to ferrocene in the cyclic voltammograms, whereas the diffusion-controlled property of the voltammograms was determined according to the literature method.[14]

[Ru(NH₃)(py^{si}S₄)] (2). Method 1: To a violet solution of **1** (450 mg, 0.38 mmol) in methanol (20 mL) was injected N_2H_4 (1 M solution in THF, 0.4 mL, 0.4 mmol) through a syringe. The solution was stirred for 25 min at room temperature. During the course of time, orange-red microcrystals were precipitated. The microcrystals were filtered, washed with methanol (20 mL) and then diethyl ether (10 mL), and dried in vacuo. Yield: 295 mg (76%). Anal. Calcd for **2** ($C_{55}H_{46}N_2RuS_4Si_2$): C, 64.73; H, 4.54; N, 2.75; S, 12.57. Found: C, 64.67; H, 4.59; N, 2.81; S, 12.49. ^{1}H NMR (269.7 MHz, CD_2Cl_2): δ 7.61 (d, $^3J_{H−H}$ = 7.1 Hz, 2 H, C_5H_3N), 7.43−7.10 (m, 31 H, $C_5H_3N/C_6H_5/C_6H_3$), 6.90−6.68 (m, 6 H, C_6H_5/C_6H_3), 4.08 (d, $^2J_{H−H}$ = 15.3 Hz, 2 H, CH_2), 3.75 (d, $^2J_{H−H}$ = 15.3 Hz, 2 H, CH_2), 1.38 (s, 3 H, NH_3). ^{13}C NMR (100.4 MHz, CD_2Cl_2): δ 166.1, 159.4, 138.5, 136.6, 136.4, 135.8, 134.3, 132.7, 130.2, 128.9, 127.7, 120.3, 120.1 ($C_5H_3N/C_6H_3/C_6H_5$), 56.7 (CH_2). IR (KBr): $\tilde\nu$ 3356,

(7) (a) Sellmann, D.; Shaban, S. Y.; Heinemann, F. W. *Eur. J. Inorg. Chem.* **2004**, 4591−4601. (b) Shaban, S. Y. Ph.D. Dissertation, University of Erlangen-Nürnberg, Erlangen, Germany, 2005.

(8) (a) Katz, N. E.; Olabe, J. A.; Aymonino, P. J. *J. Inorg. Nucl. Chem.* **1977**, *39*, 910−912. (b) Kathò, Á.; Beck, M. T. *Inorg. Chim. Acta* **1988**, *154*, 99−102. (c) Sellmann, D.; Seubert, B.; Moll, M.; Knoch, F. *Angew. Chem., Int. Ed.* **1988**, *27*, 1164−1165. (d) Chevalier, A. A.; Gentil, L. A.; Amorebieta, V. A.; Gutierrez, M. M.; Olabe, J. A. *J. Am. Chem. Soc.* **2000**, *122*, 11238−11239. (e) Gutierrez, M. M.; Amorebieta, V. A.; Estiu, G. L.; Olabe, J. A. *J. Am. Chem. Soc.* **2002**, *124*, 10307−10319.

(9) (a) Douglas, P. G.; Feltham, R. D.; Metzger, H. G. *J. Chem. Soc., Chem. Commun.* **1970**, 889−890. (b) Douglas, P. G.; Feltham, R. D.; Metzer, H. G. *J. Am. Chem. Soc.* **1971**, *93*, 84−90. (c) Bottomley, F.; Kiremire, E. M. R. *J. Chem. Soc., Dalton Trans.* **1977**, 1125−1131.

(10) (a) Bottomley, F.; Crawford, J. R. *J. Chem. Soc., Chem. Commun.* **1971**, 200−201. (b) Bottomley, F.; Crawford, J. R. *J. Am. Chem. Soc.* **1972**, *94*, 9092−9095.

(11) Prakash, R.; Czaja, A. U.; Heinemann, F. W.; Sellmann, D. *J. Am. Chem. Soc.* **2005**, *127*, 13758−13759.

(12) Enemark, J. H.; Feltham, R. D. *Coord. Chem. Rev.* **1974**, *13*, 339−406.

(13) (a) Koepp, H. M.; Wendt, H.; Strehlow, H. *Z. Elektrochem.* **1960**, *64*, 483−491. (b) Gagné, R. R.; Koval, C. A.; Lisinsky, G. C. *Inorg. Chem.* **1980**, *19*, 2854−2855. (c) Gritzner, G.; Kuta, J. *Pure Appl. Chem.* **1984**, *56*, 461−466.

(14) Bard, A. J.; Faulkner, L. R. *Electrochemical Methods, Fundamentals and Applications*; Wiley: New York, 1980.

3271, 3185, 3094 cm^{-1} ν(NH$_3$). MS (FD, THF) m/z (%): 1020 (100) [M]$^+$, 1003 (30) [M − NH$_3$], 925 (40) [M − NH$_3$ − C$_6$H$_5$]$^+$.

Method 2: To a solution of **1** (450 mg, 0.38 mmol) in methanol (20 mL) was injected N$_2$H$_4$ (1 M solution in THF, 0.8 mL, 0.8 mmol). After the solution was stirred for 10 min at room temperature, orange-red microcrystals precipitated. Yield: 322 mg (83%).

Method 3: To a solution of **1** (225 mg, 0.19 mmol) in methanol (20 mL) was added N$_2$H$_4$ (1 M solution in THF, 4.0 mL, 4.0 mmol). Instantaneously, microcrystalline **2** precipitated. Yield: 180 mg (94%).

Method 4: **1** (450 mg, 0.38 mmol) in DMF (20 mL), N$_2$H$_4$ (1 M solution in THF, 0.4 mL, 0.4 mmol); reaction time, 30 min; orange-red microcrystalline **2**. Yield: 275 mg (71%).

Method 5: **1** (450 mg, 0.38 mmol) in DMF (20 mL), N$_2$H$_4$ (1 M solution in THF, 0.8 mL, 0.8 mmol); reaction time, 10 min; orange-red microcrystalline **2**. Yield: 300 mg (78%).

Method 6: To a solution of **1** (225 mg, 0.19 mmol) in DMF (20 mL) was added N$_2$H$_4$ (1 M solution in THF, 4.0 mL, 4.0 mmol). Rapidly, microcrystals of **2** precipitated. Yield: 165 mg (86%).

[(NH$_3$)Ru(μ-py^{si}S$_4$)Ru(py^{si}S$_4$)] (3). Method 1: To a violet suspension of **1** (450 mg, 0.38 mmol) in THF (25 mL) was rapidly injected N$_2$H$_4$ (1 M solution in THF, 0.8 mL, 0.8 mmol) through a syringe. The mixture was continuously stirred for 4 h at room temperature, after which a blood-red solution developed. The solution was then filtered through a cannula, and the filtrate was concentrated (about 2 mL) under reduced pressure. The resulting gel was treated with diethyl ether (20 mL) to afford a dark-red powder. Yield: 217 mg (76%). Single crystals suitable for X-ray analysis were obtained after 10 days by the slow diffusion of Et$_2$O into a CH$_2$Cl$_2$ solution of **2**. Anal. Calcd for **3** (C$_{110}$H$_{89}$N$_3$Ru$_2$S$_8$Si$_4$): C, 65.28; H, 4.43; N, 2.08; S, 12.67. Found: C, 65.22; H, 4.40; N, 2.03; S, 12.58. ^{1}H NMR (269.7 MHz, CD$_2$Cl$_2$): δ 7.72−6.79 (m, 78 H, C$_5$H$_3$N/C$_6$H$_5$/C$_6$H$_3$), 4.14 (d, $^2J_{H-H}$ = 15.6 Hz, 2 H, CH$_2$), 3.95 (d, $^2J_{H-H}$ = 15.4 Hz, 2 H, CH$_2$), 3.76 (d, $^2J_{H-H}$ = 15.6 Hz, 2 H, CH$_2$), 3.68 (d, $^2J_{H-H}$ = 15.4 Hz, 2 H, CH$_2$), 1.41 (s, 3 H, NH$_3$). ^{13}C{^{1}H} NMR (100.4 MHz, CD$_2$Cl$_2$): δ 160−115 (many overlapping signals for C$_5$H$_3$N/C$_6$H$_5$/C$_6$H$_3$), 57.4, 57.0, 56.2, 55.7 (CH$_2$). IR (KBr): $\tilde{\nu}$ 3365, 3278, 3189, 3095 cm^{-1} ν(NH$_3$). MS (FD, THF) m/z (%): 2024 (100) [M]$^+$, 2006 (30) [M − NH$_3$]$^+$, 1020 (40) [M − Ru(py^{si}S$_4$)]$^+$.

Method 2: **1** (450 mg, 0.4 mmol) in CH$_2$Cl$_2$ (25 mL) and N$_2$H$_4$ (1 M solution in THF, 0.8 mL, 0.8 mmol); reaction time, 5 h; further workup, as above; dark-red powder **3**. Yield: 210 mg (74%).

Method 3: **1** (450 mg, 0.4 mmol) in toluene (25 mL) and N$_2$H$_4$ (1 M solution in THF, 0.8 mL, 0.8 mmol); reaction time, 12 h; further workup, as above; dark-red powder **3**. Yield: 180 mg (63%).

[Ru(NO){py^{si}S$_4$(H$^+$)}] (4). Method 1: A solution of **1** (300 mg, 0.25 mmol) in MeOH (20 mL) was stirred under an ammonia atmosphere for about 10 min at 20 °C. During this time, gray-brown microcrystals were precipitated. The microcrystals were filtered, washed with MeOH (25 mL), and dried in vacuo. Yield: 235 mg (90%). Anal. Calcd for **4** (C$_{55}$H$_{42}$N$_2$ORuS$_4$Si$_2$): C, 63.98; H, 4.10; N, 2.71; S, 12.42. Found: C, 63.89; H, 4.01; N, 2.74; S, 12.36. IR (KBr): $\tilde{\nu}$ 1826 cm^{-1} ν(NO). ^{1}H NMR (269.7 MHz, [D$_8$]THF): δ 7.50−6.80 (m, 39 H, C$_5$H$_3$N/C$_6$H$_3$/C$_6$H$_5$), 4.76 (d, $^2J_{H-H}$ = 15.7 Hz, 1H, CH$_2$), 4.66 (s, 1H, CH), 3.98 (d, $^2J_{H-H}$ = 15.6 Hz, 1H, CH$_2$). ^{13}C{^{1}H} NMR (100.4 MHz, [D$_8$]THF): δ 158−121 (26 signals, C$_5$H$_3$N/C$_6$H$_3$/C$_6$H$_5$), 53.4 (CH$_2$), 51.0 (CH). MS (FD, THF) m/z (%): 1033 (100) [M]$^+$, 1002 (45) [M − NO]$^+$, 925 (65) [M − NO − C$_6$H$_5$]$^+$.

Method 2: To a solution of **1** (300 mg 0.25 mmol) in MeOH (25 mL) was added NaN$_3$ (25 mg, 0.38 mmol), and the resulting

solution was stirred for about 1h at 20 °C. Grey-brown microcrystalline **4** precipitated. Yield: 215 mg (82%).

Protonation of 4 with HBF$_4$ to [Ru(NO)(py^{si}S$_4$)]BF$_4$ {[1$^+$]BF$_4^-$}. To a solution of **4** (200 mg 0.19 mmol) in CH$_2$Cl$_2$ was added an equimolar amount of HBF$_4$ (54% solution in Et$_2$O) at −20 °C. The solution was allowed to attain to room temperature. The dark-violet microcrystals formed were collected, washed with CH$_2$Cl$_2$ (10 mL), and dried in vacuo. IR (KBr): $\tilde{\nu}$ 1859 cm^{-1} ν(NO). ^{1}H and ^{13}C NMR: similar to that reported for **1**.[11]

X-ray Structure Analysis. A suitable single crystal was embedded in protective perfluoro polyether oil. Data were collected at T = 100 K on a Bruker-Nonius KappaCCD diffractometer using Mo K$_\alpha$ radiation (λ = 0.71073 Å) and a graphite monochromator. A semiempirical absorption correction based on multiple scans (SADABS[15]) was performed. The structure was solved by direct methods; full-matrix least-squares refinement was carried out on F^2 using SHELXTL NT 6.12. All non-hydrogen atoms were refined anisotropically. The H-atoms were geometrically positioned, with isotropic displacement parameters being 1.5 U(eq) of their corresponding C or N carrier atom. The unit cell of **3** contains approximately 1.83 CH$_2$Cl$_2$ and 2.17 Et$_2$O molecules. These solvent molecules were heavily disordered and, in part, they shared crystallographic sites. The remaining significant residual electron density maxima were all located close to the disordered solvent. Selected crystallographic data for **3**: C$_{120.52}$H$_{114.38}$Cl$_{3.65}$N$_3$O$_{2.17}$Ru$_2$S$_8$Si$_4$, crystal size 0.25 × 0.23 × 0.15 mm^3, monoclinic, space group $P2_1/n$, a = 17.336(1) Å, b = 37.357(6) Å, c = 17.580(3) Å, β = 106.221(6)°, V = 10932(3) Å^3, Z = 4, ρ_{calcd} = 1.422 g cm^{-3}, μ = 0.616 mm^{-1}, (6.7° < 2θ < 52.8°), $T_{min/max}$ = 0.935/1.000, 90 032 measured reflections, 21 101 unique reflections, 15 814 observed reflections [$I > 2\sigma(I)$], 1373 parameters, R1 = 0.0547 [$I > 2\sigma(I)$], wR2 = 0.1272 (all data).

Density Functional Theory (DFT) Calculations. All DFT calculations were performed with the program package Turbomole 5.7,[16] employing the BP86 exchange-correlation functional[17] and a triple-ζ valence-polarized Gaussian basis set.[18] A 28-electron effective core potential (ECP), which accounts for the most-important relativistic effects, was used for ruthenium.[19] The resolution of identity (RI) technique[20] was employed to accelerate the calculations. The natural population analysis (NPA)[21] was done with Gaussian03,[22] employing the Kohn−Sham molecular orbitals obtained from the Turbomole calculations. The program gOpenmol[23] was used for the visualization of the structures. All structures were fully optimized and characterized as minima on the potential energy hypersurface by means of a vibrational analysis. Accurately converged self-consistent field (SCF) results (a termination threshold of at least 1 × 10^{-8} a.u. for the total energy) were used to guarantee

(15) *SADABS 2.06*; Bruker AXS, Inc.: Madison, WI, 2002.
(16) (a) Ahlrichs, R.; Bär, M.; Häser, M.; Horn, H.; Kölmel, C. *Chem. Phys. Lett.* **1989**, *162*, 165−169. (b) For the current version, see http://www.turbomole.com.
(17) (a) Becke, A. D. *Phys. Rev. A* **1988**, *38*, 3098−3100. (b) Perdew, J. P. *Phys. Rev. B* **1986**, *33*, 8822−8824.
(18) Schäfer, A.; Huber, C.; Ahlrichs, R. *J. Chem. Phys.* **1994**, *100*, 5829−5835.
(19) Andrae, D.; Häussermann, U.; Dolg, M.; Stoll, H.; Preuss, H. *Theor. Chim. Acta* **1990**, *77*, 123−141.
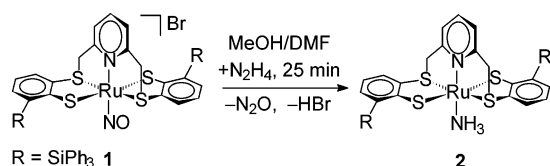(20) Eichkorn, K.; Weigend, F.; Treutler, O.; Ahlrichs, R. *Theor. Chem. Acc.* **1997**, *97*, 119−124.
(21) Reed, A. E.; Weinstock, R. B.; Weinhold, F. *J. Chem. Phys.* **1985**, *83*, 735−746.
(22) Frisch, M. J.; et al. *Gaussian 03*, revision C.02; Gaussian, Inc.: Wallingford, CT, 2004.
(23) (a) Laaksonen, L. *J. Mol. Graphics Modell.* **1992**, *10*, 33−34. (b) Bergman, D. L.; Laaksonen, L.; Laaksonen, A. *J. Mol. Graphics Modell.* **1997**, *15*, 310−306.

Scheme 1

R = SiPh₃ **1**   **2**

satisfactory accuracy in the force constant calculations. The symmetry was constrained to C_2 for complex cation $[\mathbf{1}]^+$.

Results and Discussion

The reaction of **1** with hydrazine was carried out with various ratios (1−50) of hydrazine at room temperature. The addition of an equimolar ratio of hydrazine to a violet solution of **1** in methanol caused a change in color to dark-red followed by a gas evolution (Scheme 1). When the solution was stirred for about 25 min, red microcrystalline [Ru(NH₃)(py^{si}S₄)] (**2**) precipitated in good yield (76%). The reaction was monitored by solution IR spectroscopy (Figure 1). Upon addition of hydrazine, the original NO band of **1** at 1872 cm^{-1} disappeared gradually and a new weak band at 2223 cm^{-1} appeared. The new band is consistent with the formation of N₂O,[24] and the evolved N₂O gas was further confirmed by GC/MS analysis (Figures 1S and 2S, Supporting Information). Because of the highly air-sensitive nature of the complexes and the complicated experimental setup, it was not possible to determine the accurate quantity of N₂O produced (in the gas phase as well as in solution) during the reaction. Nevertheless, because of the amount of **1** and hydrazine used to the amount of **2** produced, the stoichiometry of the reaction can be recognized as 1:1:1. When the ratio of hydrazine was doubled, the NO band of **1** vanished within 10 min and the ammonia complex was isolated in 83% yield. With excess hydrazine concentrations (20−50 times), the reaction was very rapid and microcrystals of **2** formed instantaneously. Analogous experiments performed in DMF afforded identical results. But in none of these reactions was the formation of hydrazine complex observed.

Moreover, the IR spectra (Figure 1) did not show any new band in the regions between 2200 and 1900 cm^{-1} or 1700−1600 cm^{-1}, which suggests that no azide (either free or in coordinated form) or one-electron reduced (19-valence-electron) neutral nitrosyl complex [Ru(NO)(py^{si}S₄)]⁰ ({Ru−NO}⁷) was produced during the reaction. On the other hand, the cyclic voltammogram of **1**[11] suggested that the species {Ru−NO}⁷ exists in solution at approximately 0.0 V vs NHE. However, attempts to generate the species by chemical as well as electrochemical methods remained unsuccessful. So far, only in the case of the related iron compound [Fe(NO)(pyS₄)]⁺ {pyS₄²⁻ = 2,6-bis(2-sulfanyl-phenylthiomethyl)pyridine²⁻} ({Fe−NO}⁶) was such a one-electron reduction achieved with hydrazine, and the resulting {Fe−NO}⁷complex was isolated in the solid state.[25] This
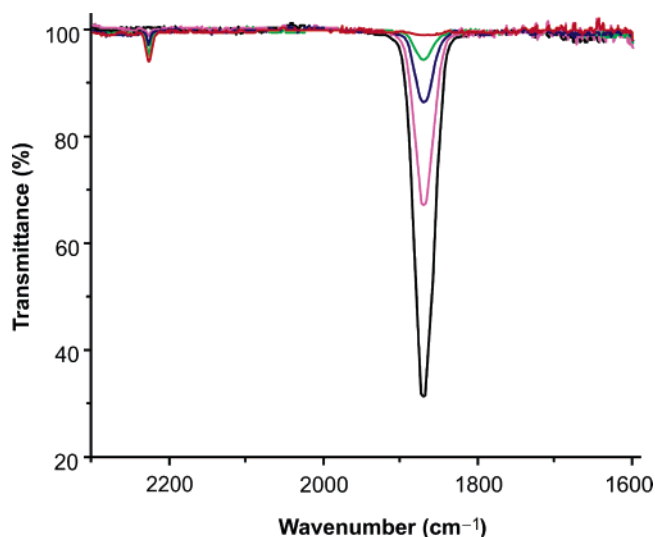

Figure 1. IR spectroscopic monitoring of the reaction between an equimolar ratio of **1** and hydrazine in methanol at 20 °C. Complex **1** without (black) and with hydrazine after 6 min (magenta), 12 min (blue), 18 min (green), and 25 min (red).

suggests that the reactivity of NO⁺ depends largely on the metal as well as on the coligand environment, which influences the electron density of the nitrosyl ligand.

Complex **2** is soluble in THF, CH₂Cl₂, CHCl₃, and toluene. The IR (KBr) spectrum of **2** displays sharp bands at 3356, 3271, 3185, and 3094 cm^{-1} assignable to ν(NH) of the NH₃ ligand, which is characteristic for thiolate−ruthenium−ammine complexes.[26] The well-resolved ^{1}H and ^{13}C NMR spectra of **2** indicate its ground-state spin is zero. The observed resonances (see Experimental Section) are typical for the C_2 symmetric [Ru(py^{si}S₄)] fragment.[11] The cyclic voltammogram of **2** exhibits a reversible one-electron wave at $E_{1/2} = 0.255$ V vs NHE, which is assigned to the Ru$^{II/III}$ redox couple (Figure 3S, Supporting Information). The couple is reversible on the basis of its similarity to ferrocene in the cyclic voltammogram. The peak current increases linearly with the square root of the scan speeds, indicating that the redox reaction is a diffusion-controlled process. Moreover, in multisweep experiments under thin-layer conditions, the redox wave revealed complete reversibility over several cycles, suggesting that the Ru−NH₃ bond is intact during oxidation.

In the solid state under an N₂ atmosphere at ambient temperature, **2** is stable for a prolonged period of time; however, in solution (THF, CH₂Cl₂, CHCl₃, or toluene), it dimerizes after 2 days and forms dinuclear ammine complex **3** (Scheme 2). Because the CH₂ protons are good NMR probes, the reaction could be monitored by ^{1}H NMR spectroscopy (Figure 2). The two doublet signals of the diastereotopic protons of C_2 symmetric **2** changed into four doublets, which corresponds to the CH₂ protons of C_1 symmetric complex **3**. When the solution of **3** is stirred under

(24) For ν(N₂O) in solution, see: (a) Gorga, J. C.; Hazzard, J. H.; Caughey, W. S. *Arch. Biochem. Biophys.* **1985**, *240*, 734−746. (b) Hu, T. A.; Chappell, E. L.; Sharpe, S. W. *J. Chem. Phys.* **1993**, 98, 6162−6169.
(25) Sellmann, D.; Blum, N.; Heinemann, F. W. *Chem.—Eur. J.* **2001**, *7*, 1874−1880.

(26) (a) Sellmann, D.; Prakash, R.; Heinemann, F. W. *Eur. J. Inorg. Chem.* **2004**, 4291−4299. (b) Sellmann, D.; Hille, A.; Rösler, A.; Heinemann, F. W.; Moll, M.; Brehm, G.; Schneider, S.; Reiher, M.; Hess, B. A.; Bauer, W. *Chem.—Eur. J.* **2004**, 10, 819−830. (c) Sellmann, D.; Hein, K.; Heinemann, F. W. *Eur. J. Inorg. Chem.* **2004**, 3136−3146.
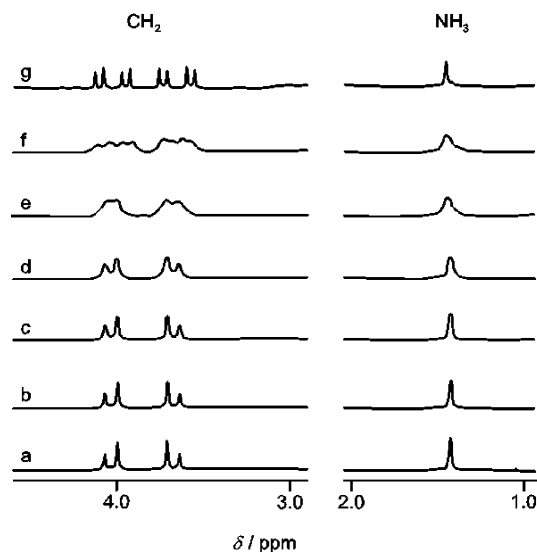
Figure 2. ^{1}H NMR spectroscopic monitoring of the conversion of **2** to **3** in CD$_2$Cl$_2$ under N$_2$ at 20 °C. Only the region between $\delta = 4$ and $\delta = 1$ is shown. Time intervals are (a) 1, (b) 10, (c) 20, (d) 30, (e) 40, (f) 50, and (g) 60 h.
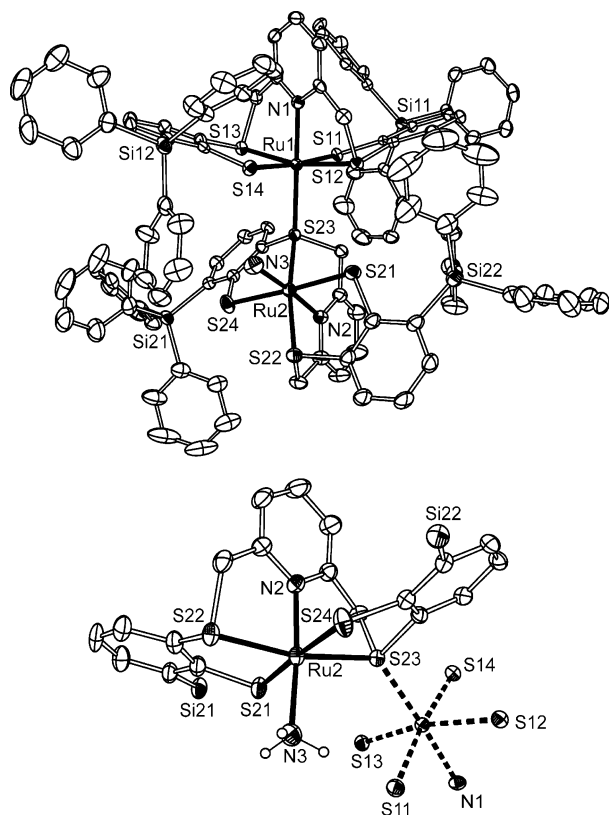

Figure 3. Top: Molecular structure of **3** (50% probability level ellipsoids; H atoms and solvent molecules omitted). Bottom: SiPh$_3$ phenyl groups of the Ru2 fragment and the ligand unit, except core atoms around Ru1 are omitted.

an ammonia atmosphere for about 6 h, the mononuclear compound **2** is formed again. Consequently, several attempts to grow single crystals of **2** suitable for X-ray analysis, even in some cases under an atmosphere of ammonia, inevitably yielded only crystals of dinuclear complex **3**.

This result prompted us to study the reaction in less-polar (THF and CH$_2$Cl$_2$) as well as nonpolar (toluene) solvents.
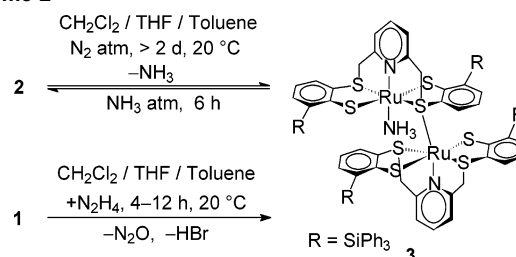
Scheme 2

Table 1. Selected Bond Distances (Å) and Angles (deg) for **3**·1.83CH$_2$Cl$_2$·2.17Et$_2$O

Ru1−N1	2.064(3)	N1−Ru1−S11	89.20(9)
Ru1−S11	2.373(2)	N1−Ru1−S23	177.30(9)
Ru1−S12	2.323(1)	S11−Ru1−S12	86.94(4)
Ru1−S13	2.311(1)	S11−Ru1−S14	174.12(4)
Ru1−S14	2.399(2)	S12−Ru1−S13	165.51(4)
Ru1−S23	2.354(1)	N2−Ru2−N3	175.1(2)
Ru2−N2	2.030(3)	N2−Ru2−S21	91.0(1)
Ru2−N3	2.138(4)	S21−Ru2−S22	86.84(4)
Ru2−S21	2.360(2)	S21−Ru2−S24	177.42(4)
Ru2−S22	2.307(2)	S22−Ru2−S23	166.26(4)
Ru2−S23	2.315(2)	Ru1−S23−Ru2	131.26(4)
Ru2−S24	2.382(2)		

In contrast to the observation made in MeOH/DMF, the addition of hydrazine to a suspension of **1** in THF (or CH$_2$Cl$_2$) did not cause any immediate color change or solution formation. A clear red solution formed only when the suspension was stirred for more than 4 h at room temperature. In toluene, the reaction had to be prolonged for 12 h to get the red solution. The IR spectrum of the resulting solution in all cases displayed only a weak band at 2224 cm^{-1}, indicating that the one-electron reduced neutral nitrosyl complex or azide complex was not formed. Further workup of this solution directly afforded dinuclear ammine complex [(NH$_3$)Ru(μ-py^{si}S$_4$)Ru(py^{si}S$_4$)] (**3**) in good yield (Scheme 2).[27] The IR (KBr) spectrum of **3** exhibits sharp ν(NH$_3$) bands at 3365, 3278, 3189, and 3095 cm^{-1}, which are slightly blue-shifted when compared to those of **2**. ^{1}H and ^{13}C NMR spectra of **3** suggest that the complex has C_1 symmetry, which has also been confirmed by an X-ray structure analysis. **3** exhibits two one-electron reversible (with respect to the ferrocene couple) waves at $E_{1/2} = 0.228$ and 0.780 V vs NHE (Figure 4S, Supporting Information). These waves can be assigned to the two Ru$^{II/III}$ redox couples of **3**, which show complete reversibility over several successive cycles.

The molecular structure of **3** is depicted in Figure 3, and selected distances and angles are given in Table 1. Complex **3** crystallizes in the monoclinic space group $P2_1/n$.[28] Each ruthenium (Ru1, Ru2) center exhibits a distorted octahedral coordination geometry comprised of one nitrogen and four sulfur donor atoms of the ligand py^{si}S$_4^{2-}$. The sixth coor-

(27) The reaction between **1** and hydrazine (>20 equiv) in THF (CH$_2$Cl$_2$ or toluene) yielded a mixture that could not be separated even by chromatography. However, crystallization of the mixture exclusively yielded the crystals of **3**.

(28) CCDC 255036 (**3**) contains supplementary crystallographic data for this paper. These data can be obtained free of charge via www.ccdc.cam.ac.uk/conts/retrieving.html (or from the Cambridge Crystallographic Data Centre, 12, Union Road, Cambridge CB21EZ, U.K.; fax: (44) 1223-336-033; or deposit@ccdc.cam.ac.uk).

dination site of Ru2, trans to the pyridine N atom, is occupied by the NH_3 ligand. The thioether donor S23 of the Ru2 unit bridges the Ru1 fragment. In this respect, complex **3** differs distinctly from many of our common dinuclear complexes, where two thiolate donors exclusively bridge two metal centers.[29] The thiolate and thioether donors occupy trans position to each other. The distances around ruthenium, including the $Ru-NH_3$ bond, are in the range usually found for the diamagnetic octahedral Ru^{II}-thiolate-thioether complexes.[26,29] The bridging Ru1-S23 bond length is distinctly shorter than even the Ru-S (thiolate) distances; however, it coincides with the value that is reported for known ruthenium-thioether-bridged complexes.[30] The Ru1-S23-Ru2 angle of 131.26(4)° may be due to steric effects caused by the bulky $SiPh_3$ groups.

Alternatively, electrochemical reductions of coordinated nitrosyls to coordinated ammonia in aqueous solution have been reported for a variety of polypyridyl complexes of both ruthenium and osmium.[31] The mechanism involves a series of facile one-electron-transfer steps. Therefore, efforts have been made to electrochemically convert **1** to **2**. The cyclic voltammogram of **1** exhibits the NO^0/NO^{-1} reduction wave at $E_{1/2} = -1.25$ V vs NHE, which is irreversible. No other redox wave was observed up to -1.8 V. Constant potential coulometric reactions were carried out with **1** in the presence of protons in CH_2Cl_2 at -1.05 V vs SCE.[32] No ammonia or ammine complex was formed, and the reaction yielded only a brown solid that cannot yet be characterized. Thus, the electrochemical reduction of the bound NO^+ of **1** to NH_3 seems to be impossible under this condition.

Unlike in the reaction with hydrazine, **1** reacts readily with other N-donor nucleophiles such as ammonia and azide in methanol at 20 °C to exclusively give the neutral nitrosyl complex $[Ru(NO)\{py^{si}S_4(-H^+)\}]$ (**4**) in very high yields (Scheme 3).[33] This finding precludes the formation of **2** and **3** from **1** and ammonia as an intermediary decomposition product of hydrazine. The IR (KBr) spectrum of **4** exhibits a sharp $\nu(NO)$ band at 1826 cm^{-1}. When compared to **1**, the NO band of **4** is red-shifted by 32 cm^{-1}. This is in good agreement with the values that are reported for the loss of a

Scheme 3

R = SiPh$_3$ **1**

(a) + NH$_3$, 10 min
−NH$_4$Br

MeOH

(b) + NaN$_3$, 1 h
−HN$_3$, −NaBr

4
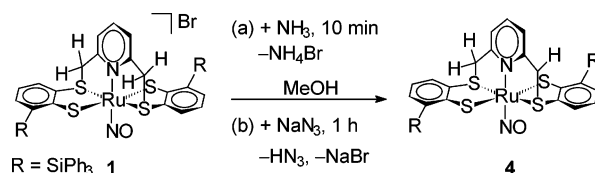
proton from similar thiolate−thioether complexes.[34] The ^{1}H NMR spectrum of **4** (see Experimental Section) indicated that the deprotonation occurred at one of the bridging CH_2 protons. It has already been proven that the bridging CH_2 protons of **1** are more acidic, because of the electron-withdrawing effect of the NO^+ ligand, and undergo H^+/D^+ exchange with CD_3OD.[11] The cyclic voltammogram of **4** exhibits two one-electron reversible (with respect to the ferrocene couple) waves at $E_{1/2} = 0.42$ and −0.56 V vs NHE for the redox couples of $[4]^{-1/0}$ and $[4]^{-1/-2}$, respectively. This is in concurrence with **1**,[11] indicating that the 19-valence-electron anionic species $[Ru(NO)\{py^{si}S_4(-H^+)\}]^-$ exists in solution at approximately −0.1 V. When the CV of **4** is compared with that of **1**, the half-wave potentials of the corresponding peaks of **4** are shifted to more-negative values. Protonation of **4** with HBF_4 in CH_2Cl_2 at −20 °C led to the regeneration of $[1]^+$ with BF_4 as counterion. These results obviously confirmed that both NH_3 and N_3^- acted simply as bases to deprotonate one of the highly acidic $-CH_2$ protons rather than as nucleophiles.

To corroborate the experimental findings, DFT calculations were carried out for $[1]^+$ and its deprotonation product **4** (Table 1S and Figure 5S, Supporting Information). The theoretical structure determination (geometry optimization) yielded bond distances and bond angles in very good agreement with the X-ray structure determination of $[1]^+$ (Table 1S, Supporting Information), which underlines the reliability of the calculations. The deprotonation at one of the bridging CH_2 groups is accompanied by distinct structural changes in the framework of the $py^{Si}S_4$ ligand (see the Supporting Information) and a slight elongation of the NO bond length. A natural population analysis did not reveal any significant differences in the natural atomic charges of individual atoms between $[1]^+$ and **4**. The charge is rather uniformly distributed over the $py^{Si}S_4$ ligand; deprotonation simply frees up more electron density for a better back-bonding to the NO ligand, which is reflected by a reduction of the natural charge of the NO ligand by 0.08e. The calculation of the harmonic force fields for $[1]^+$ and **4** resulted in a red-shift of 34 cm^{-1} for the $\nu(NO)$ band upon deprotonation. This is in perfect agreement with the experimentally observed value of 32 cm^{-1} and thus proves the formation of **4** upon reaction of $[1]^+$ with NH_3 or N_3^-.

The reaction of **1** with hydrazine is interesting because of the formation of N_2O as one of the products, which is not a common product of hydrazine oxidation.[6] In addition, **2** cannot be obtained directly from the reaction between **1** and NH_3. Thus, it is obvious that complex **1** underwent nitrosation

(29) (a) Sellmann, D.; Prakash, R.; Heinemann, F. W.; Moll, M.; Klimowicz, M. *Angew. Chem., Int. Ed.* **2004**, *43*, 1877−1880. (b) Sellmann, D.; Sutter, J. *Prog. Inorg. Chem.* **2003**, *52*, 585−681.
(30) (a) Shin, R. Y. C.; Ng, S. Y.; Tan, G. K.; Koh, L. L.; Khoo, S. B.; Goh, L. Y.; Webster, R. D. *Organometallics* **2004**, *23*, 547−558. (b) Grapperhaus, G. A.; Poturovic, S.; Mashuta, M. S. *Inorg. Chem.* **2002**, *41*, 4309−4311.
(31) (a) Armor, J. N.; Hofmann, M. Z. *Inorg. Chem.* **1975**, *14*, 444−446. (b) Murphy, W. R., Jr.; Takeuchi, K. J.; Meyer, T. J. *J. Am. Chem. Soc.* **1982**, *104*, 5817−5819. (c) Murphy, W. R., Jr.; Takeuchi, K. J.; Barley, M. H.; Meyer, T. J. *Inorg. Chem.* **1986**, *25*, 1041−1053.
(32) Constant potential coulometric reductions were performed in a gastight coulometric cell with a Pt working electrode, a platinum wire counter and a SCE reference electrode. [Complex] = 1 mM; [H$^+$] = 3−10 mM; [NBu$_4$PF$_6$] = 0.1 M; CH_2Cl_2 = 50 mL. Applied potential = −1.05 V vs SCE; SCE = +234 V with respect to NHE.[14] In all experiments, the pink suspension of **1** was changed to brown 30−60 min after consuming coulombs nearly equivalent to 2−3 electrons. Gas samples taken before and after the electrolysis were analyzed for NH_3.
(33) Only complex **4** is formed, regardless of solvents (polar or nonpolar) and concentrations of the nucleophiles used. The HN_3 showed a sharp IR band at 2131 cm^{-1} in methanol.
(34) Sellmann, D.; Utz, J.; Blum, N.; Heinemann, F. W. *Coord. Chem. Rev.* **1999**, *190−192*, 607−627.

Scheme 4
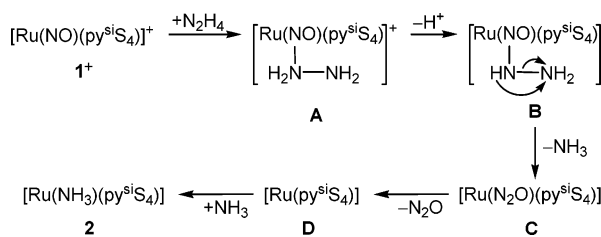
ith hydrazine to form **2** and N_2O. The plausible mechanism for the hydrazine nitrosation is given in Scheme 4, which is similar to the one that was proposed earlier.[7d] It involves the initial nucleophilic addition of N_2H_4 on the nitrosyl nitrogen of **1** to form a labile adduct **A**, which rapidly deprotonates at the bond-forming nitrogen of hydrazine (**B**). The stoichiometry requires the second proton to migrate to the remote N-atom of hydrazine, followed by the cleavage of the N−N bond in the hydrazine-derived moiety, resulting in $[Ru(N_2O)(py^{si}S_4)]$ (**C**) and NH_3. Subsequent release of the N_2O from **C** leads to the formation of an unstable five-coordinate fragment $[Ru(py^{si}S_4)]$ (**D**). Because of the steric effect of the $SiPh_3$ groups in the vicinity of the thiolate donors, a dimerization of the fragment **D** through thiolate bridges is not favorable. In the final step, the NH_3 is coordinated into the vacant site of **D** to give **2**.

The different modes of NO^+ reactivity of Fe, Ru, and Os complexes toward hydrazine may directly be related to the metal and coligand environment, which influences the electron density of the nitrosyl ligand through $\sigma-\pi$ interactions.[35] After the removal of two protons from the coordinated N atom of the hydrazine, most rutheniumnitrosyls facilitate the proton loss from the terminal nitrogen atom of hydrazine and the subsequent removal of water, leading to azide complexes. Whereas the reactivity of complex **1** closely resembles the iron nitrosyl complex $[Fe(NO)(CN)_5]^{2-}$,[7d] the protons in the terminal nitrogen atom are retained and ammonia is released after a heterolytic cleavage of the N−N

bond. The one-electron reduced neutral nitrosyl complex $[Ru(NO)(py^{si}S_4)]^0$ (${Ru-NO}^7$) is not detected during this reaction, which suggests that the bound NO^+ underwent two-electron reduction to form N_2O. To our knowledge, **1** seems to be the first ruthenium nitrosyl complex to yield nitrous oxide and ammonia upon hydrazine nitrosation, according to Stedman's prediction in nonacidic medium.[6]

Conclusion

In this paper, we have described the nitrosation reaction of $[Ru(NO)(py^{si}S_4)]Br\cdot THF$ (**1**) with hydrazine in various nonaqueous solvents. The reaction carried out in polar solvents such as methanol and DMF afforded mononuclear $[Ru(NH_3)(py^{si}S_4)]$ (**2**) and N_2O, whereas in less polar solvents such as THF, CH_2Cl_2 and toluene dinuclear $[(NH_3)Ru-(\mu-py^{si}S_4)Ru(py^{si}S_4)]$ (**3**) formed in high yield. The X-ray structure analysis indicated that in complex **3**, the two $[Ru(py^{si}S_4)]$ fragments are bridged by a thioether donor. Complex **2** dimerizes in solution to give **3**, and the reverse reaction was achieved by treatment of **3** with NH_3. On the contrary, reaction of **1** with NH_3 as well as N_3^- merely yielded the neutral nitrosyl complex $[Ru(NO)\{py^{si}S_4(-H^+)\}]$ (**4**). A plausible mechanism for the hydrazine nitrosation of **1** has been proposed. The reactivity of **1** toward hydrazine differs remarkably from other rutheniumnitrosyls, which might be due to the fine-tuning effect of the thioether−thiolate donors of the chelate ligand. Efforts are currently underway to explore the reactivity features of **1** with various other nucleophiles.

Supporting Information Available: GC/MS spectra, cyclic voltammograms, additional results from the DFT calculations, complete list of authors in ref 22, crystallographic data for **3** in CIF format. This material is available free of charge via the Internet at http://pubs.acs.org.

(35) Callahan, R. W.; Meyer, T. J. *Inorg. Chem.* **1977**, *16*, 574−581.

IC060096J